CHIN. PHYS. LETT. Vol. 29, No. 2 (2012) 020701

Fabrication and Performance of Micro-sensors for Methane Detection Based on In-Pd-Co-SnO_2 Composite Nanofibers *

QIAO Ji-Ping(乔记平)[1,2], ZHU Zi-Peng(朱子鹏)[1], YAN Xiao-Yan(闫晓燕)[3], QIN Jian-Min(秦建敏)[2**]

[1] *College of Physics & Optoelectronics, Taiyuan University of Technology, Taiyuan 030024*
[2] *Institute of Measuring and Controlling Technology, Taiyuan University of Technology, Taiyuan 030024*
[3] *School of Electronics and Computer Science & Technology, North University of China, Taiyuan 030051*

(Received 21 September 2011)

In-Pd-Co-SnO_2 composite nanofibers have been synthesized by an electrospinning method and characterized by x-ray diffraction (XRD), scanning electron microscopy (SEM), and transmission electron microscopy (TEM). Micro-sensors with a tiny area of $1\times1\,mm^2$ are fabricated by spinning the nanofibers on sensor substrates. Excellent CH_4 sensing properties are found based on the micro-sensors. The sensitivity is up to 13 when the sensors are exposed to 10 ppm CH_4 at 140°C, and the response and recovery times are about 8 and 14 s, respectively. High selectivity, good stability, and low power-consumption are also observed in the investigation.

PACS: 07.07.Df, 82.47.Rs DOI:10.1088/0256-307X/29/2/020701

Methane (CH_4) is a volatile gas with a high explosion probability for its ready inflammability. This gas can displace oxygen to cause asphyxiation in cramped or inadequately ventilated areas. It has also been proved to be about a 20 times more effective greenhouse warming-gas than carbon dioxide.[1] Therefore, developing methane sensors has gained a special focus driven by this application. Semi-conducting metal oxides like SnO_2, ZnO, In_2O_3, and Fe_2O_3 have been used to detect toxic and explosive gases for more than four decades.[2–4] However, two shortages often limit their sensing applications. First, these oxides exhibit responses to many gases, thus show a poor selectivity.[5] For the high selectivity of methane detection, at least two or three dopants are usually needed, which are reported to be Pd, Fe, In, Co, etc.[6] Second, the traditional semi-conducting sensing materials are nanopowders, which suffer from a degradation because of aggregation growth among nanopowders. In particular, the sensors operating at high temperatures will promote this aggregation effect and eventually lead to a poor stability.[7]

In this Letter, we report micro-sensors fabricated from semi-conducting techniques and electrospinning methods. The sensor substrates with a small area ($1 \times 1\,mm^2$) are obtained by sputtering Pt-Ti electrodes on Si chips. The sensing materials are In-Pd-Co-SnO_2 composite nanofibers, which are prepared by electrospinning a precursory solution of $SnCl_2{\cdot}2H_2O$, ethanol, N,N-dimethylformamide, poly(vinyl pyrrolidone), $In(NO_3)_3$,etc. The obtained micro-sensors exhibit excellent methane sensing properties, which have high sensitivity, quick response and recovery, high selectivity, good stability and low power-consumption. The results show the potential application of this type of micro-sensor for methane detection in practice.

In-Pd-Co-SnO_2 composite nanofibers were synthesized via a simple electrospinning method. Typically, 0.385 g of $SnCl_2{\cdot}2H_2O$ was mixed with 4.5 g of N,N-dimethylformamide and 4.5 g of ethanol in a glovebox under vigorous stirring for 6 h. Subsequently, this solution was in turn added to 0.8 g of poly(vinyl pyrrolidone) (PVP, Mw = 1300000), $In(NO_3)_3$ (0.12 g), $PdCl_2$ (0.08 g), and $Co(NO_3)_2{\cdot}6H_2O$ (0.04 g) under vigorous stirring for 10 h. The obtained solution was then loaded into a glass syringe in which the internal diameter of the pinhead is 0.8 mm. The pinhead was connected to a high voltage supply that was capable of generating direct current voltages of up to 30 kV. In our experiment, a voltage of 12 kV was applied for electrospinning. An aluminum foil served as the substrate electrode, and the distance between the pinhead and the substrate electrode was 20 cm. In order to remove PVP completely, the precursory nanofibers were calcined in air at 600℃ for 2 h. Then, In-Pd-Co-SnO_2 composite nanofibers were obtained.

The crystal structures of the products were determined by x-ray powder diffraction (XRD) using an x-ray diffractometer (Siemens D5005, Munich, Germany) with Cu Kα radiation ($\lambda = 1.5418$ Å). Scanning electron microscopy (SEM) images were recorded on a SHIMADZU SSX-550 (Japan) instrument. Transmission electron microscopy (TEM) images were obtained on a JEOL JEM-2000EX microscope with an accelerating voltage of 200 kV.

Micro-sensors were fabricated by spinning In-Pd-Co-SnO_2 composite nanofibers on sensor substrates. The structure and electrode design of the sensor substrates are shown in Fig. 1(a). The substrates were achieved according to the following steps: (a) growing SiO_2 (with a thickness of 2000 Å) on the two sides of Si wafers as the insulating layer, (b) sputtering a Ti layer (with a thickness of 200 Å, adhering layer) and a Pt layer (with a thickness of 1800 Å) on SiO_2 layers as metal electrodes, (c) mask patterns transfer to the Si wafer by photolithography, (d) etching the Ti and Pt layers to form signal electrodes and heater electrodes by reactive ion etching, (e) removing the

*Supported by the Natural Science Basic Research Plan of Shanxi Province under Grant No 2010011026-2.
**Email: qinjianmintaiyuan@163.com

photoresist, (f) cutting Si wafers to form sensor substrates. A top view (obtained in a microscope) and the electrode design of the micro sensors are shown in Fig. 2(a). The width and distance of the sensor electrodes are 25 μm, and the surface area of the sensors is about $1 \times 1\,\mathrm{mm}^2$. Sensing films were obtained by laying sensor substrates on the aluminum foil in the electrospinning process, and spinning In-Pd-Co-SnO_2 precursory jets for 4 h. Then the substrates were calcined at 600℃ for 2 h to convert precursory jets to In-Pd-Co-SnO_2 composite nanofibers. Figure 2(b) shows a comparison between a socketed micro-sensor and a Chinese coin (1 Yuan).

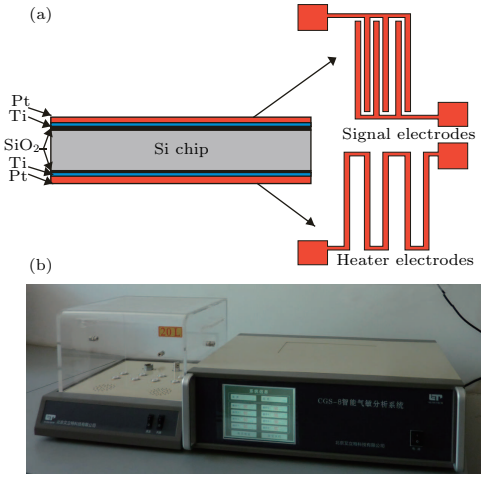

Fig. 1. (a) Structure and electrode design of the sensor substrates, (b) a photograph of the sensing measurement.

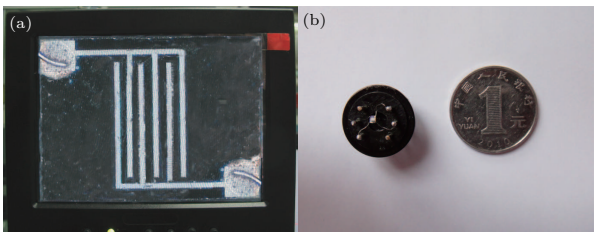

Fig. 2. (a) A photograph of a sensor substrate (top view) obtained in a microscope, (b) comparison between a socketed micro-sensor and a Chinese coin (1 Yuan).

The sensor performances were measured by a CGS-8 (Chemical Gas Sensor-8) intelligent gas sensing analysis system (Beijing Elite Tech Co., Ltd, China) (Fig. 1(b)). This system could provide various operating currents to control the sensor temperature (measured by a Testo 845 infrared thermometer (TESTO AG, Germany)). Gas ambiences were obtained by a static test system.[2] A suitable volume of target vapor or liquid was injected into the test chamber (20 L in volume for CGS-8 in this case) by a syringe through a rubber plug. For a gas prepared by vapor sources, the source volume was calculated by $Q = C \times V$, where Q is the volume value, C is the target concentration, and V is the chamber volume. If a liquid was used as the gas source, the volume was calculated by $Q = (C \times V \times M)/(22.4 \times d \times p)$, where Q is the liquid volume, C is the target concentration, V is the chamber volume, M is the molecular weight, d is the density, p is the purity. In particular, all the sensors were pre-heated at different operating temperatures for about 30 min. When the resistances of the sensors were stable, an appropriate volume of target gas or liquid was injected into the test chamber, and then mixed with air by two fans in the analysis system. After the sensor resistances reached new constant values, the test chamber was opened to recover the sensors in air. The whole experiment process was performed with a constant humidity (25% RH) and temperature (20℃).

The sensitivity value S was designated as $S = R_a/R_g$, where R_a is the sensor resistance in air (base resistance) and R_g is a mixture of target gas and air. The time taken by the sensor resistance to change from R_a to $R_a - 90\% \times (R_a - R_g)$ is defined as the response time when the target gas is introduced to the sensor, and the time taken from R_g to $R_g + 90\% \times (R_a - R_g)$ is defined as the recovery time when the ambience is replaced by air.

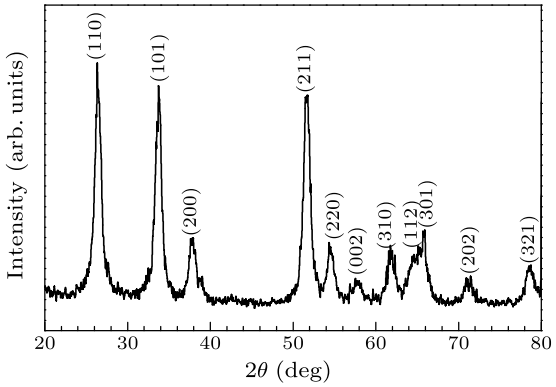

Fig. 3. XRD pattern of In-Pd-Co-SnO_2 composite nanofibers.

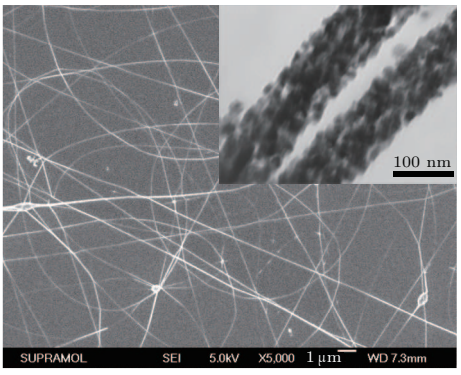

Fig. 4. SEM and TEM (inset) images of In-Pd-Co-SnO_2 composite nanofibers.

Figure 3 shows the XRD pattern obtained from In-Pd-Co-SnO_2 composite nanofibers. The prominent peaks corresponding to (110), (101) and (211) crystal lattice planes and all other smaller peaks coincide with the corresponding peaks of the rutile structure of SnO_2 given in the standard data file (JCPDS File No. 41-1445). No other characteristic peaks corresponding to the dopants are observed, which is because of

the very low content of these dopants in the composite nanofibers.

Figure 4 shows the SEM image of In-Pd-Co-SnO_2 composite nanofibers. The product is highly dominated by the nanofibers with lengths of several tens of micrometers and diameters ranging from 60 to 140 nm. The average diameter of the nanofibers is about 100 nm. The TEM image of two nanofibers (insert in Fig. 4) shows that the nanofibers are formed by well-regulated nanoparticles with an average diameter of about 20 nm.

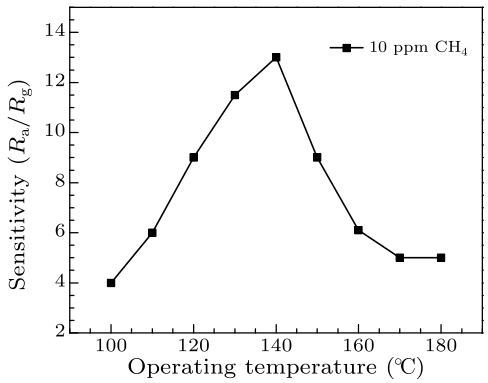

Fig. 5. Sensitivities of the micro-sensors to 10 ppm CH_4 at different operating temperatures.

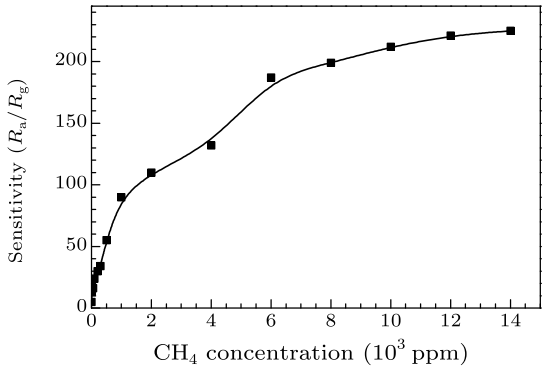

Fig. 6. Sensitivities of micro-sensors to different CH_4 concentrations at 140℃.

Gas sensing measurements are performed at different operating temperatures to find the optimum operating condition. Figure 5 shows the relationship between different operating temperatures and the sensor sensitivities of the sensors to 10 ppm CH_4. The sensitivity increases and reaches its maximum at 140℃, and then decreases rapidly with increasing temperature. This tendency is commonly observed for many semi-conducting metal oxide-based sensors, and can be explained by considering the surface coverage of the oxygen adsorbate at the steady-state.[8] Higher temperatures can improve the activation of oxygen adsorbate, but decrease the surface coverage rate. In this case, the optimum operating temperature is found to be 140℃. The power-consumption of the current sensors at this operating temperature is only about 40 mW, and the value is much lower than those of many semi-conducting metal oxide-based sensors reported before.

The sensitivities of the micro-sensors to different CH_4 concentrations at 140℃ are shown in Fig. 6. When exposed to 1 ppm CH_4, the sensitivity of the sensor is up to 5. With increasing CH_4 concentration, the sensitivity increases significantly. For CH_4 at level of 10, 50, 100, 300, 500, 1000, 2000, 4000, and 8000 ppm, the sensitivity is about 13, 16, 24, 34, 55, 90, 110, 132, and 199, respectively. The low detection limit (below 1 ppm) with high saturated concentration (about 12000 ppm) of current CH_4 micro-sensors suggests that these sensors are good candidates for CH_4 detection with a large measuring range.

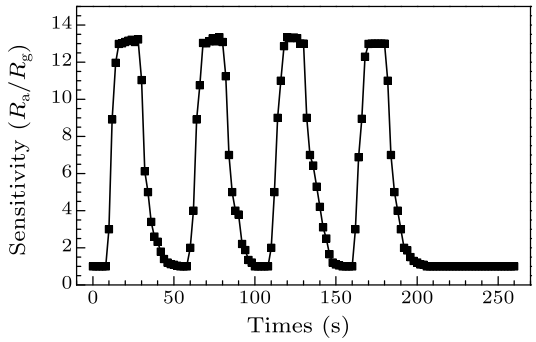

Fig. 7. Response-recovery curves of micro-sensors to 10 ppm CH_4 at 140℃.

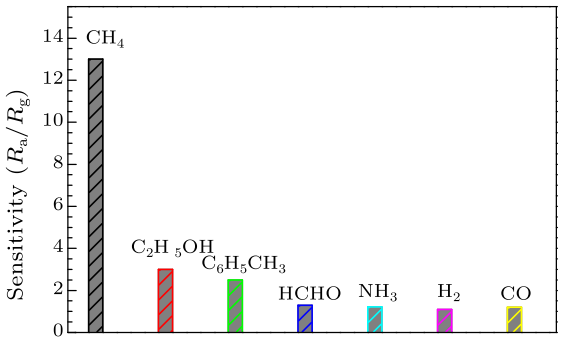

Fig. 8. Selectivity of micro-sensors at 140℃.

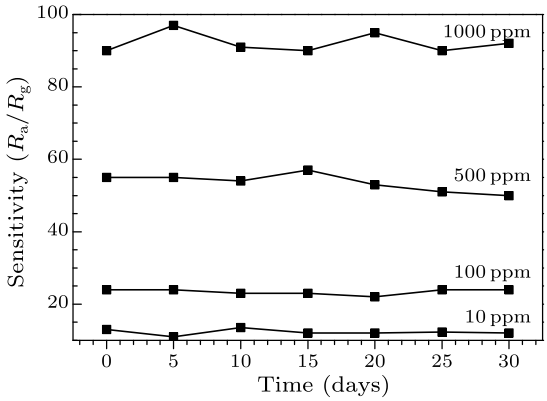

Fig. 9. Long-time stability of micro-sensors to 10, 100, 500 and 1000 ppm CH_4.

Response-recovery curves of the micro-sensors to 10 ppm CH_4 are shown in Fig. 7. In the measure-

ments, four periods were examined at 140℃. The response and recovery times are found to be about 8 and 14 s, respectively. Such quick speeds are based on the structures of as-prepared fibers. The large surface of the SnO_2 nanofibers makes the absorption of CH_4 molecules on the surface of the material easy. The one-dimensional structures of the fibers can facilitate fast mass transfer of the CH_4 molecules to and from the interaction region as well as improve the rate for charge carriers to transverse the barriers induced by molecular recognition along the fibers.[9] In addition, the fabricating techniques of the micro-sensor hurtles to the nanostructure of the nanofibers because no-coating process is used.[10] Therefore, the web-like structure can naturally be formed on the sensor surface,[11] which can greatly enhance the absorption and desorption of the micro-sensors, and eventually lead to short response and recovery times.

The selectivity of the micro-sensors at 140℃ is shown in Fig. 8. The gas concentration is controlled at 10 ppm in each test. High selectivity is observed because the sensitivity of the sensors to CH_4 is much greater than that of the sensors to C_2H_5OH, $C_6H_5CH_3$, HCHO, NH_3, H_2, and CO. This result suggests that the current micro-sensors can be used for CH_4 detection in various atmospheres.

The long-time stability of the micro-sensors has also been measured as shown in Fig. 9. The sensors exhibit a nearly constant sensor signal to 10, 100, 500 and 1000 ppm CH_4 in the tests, confirming a good stability of the micro-sensors.

The sensing mechanism for SnO_2 based chemical sensors has been described in the literature by many authors. Basically, the electrical change of SnO_2 related sensing materials is primarily caused by adsorption and desorption of gas molecules on the surface of the sensing film. When SnO_2 nanofibers are surrounded by air, oxygen molecules can adsorb on the fiber surface, and catch electrons to generate chemisorbed oxygen species (O^- is believed to be dominant). Therefore, the micro-sensors will show a high resistance. When the SnO_2 nanofibers are exposed to a reducing gas at an appropriate temperature (such as CH_4 at 140℃ in this case), the reducing gas reacts with the adsorbed oxygen molecules and releases the trapped electrons back to the conduction band, thereby increasing the conductivity of SnO_2. The effects of the dopants in current SnO_2 nanofibers are complicated and a possible mechanism is provided as follows. In_2O_3 is also a topical sensing material, which has sensitivities to both reducing (e.g., C_2H_5OH, CO, CH_4, and H_2) and oxidizing gases (e.g., NO_X). In the SnO_2-In_2O_3 system, it is believed that replacement of some Sn^{4+} by In^{3+} ions with a lower valence can enhance the active surface states for the adsorption of detecting gases and benefit its sensing properties. Since trivalent In^{3+} acts as an acceptor impurity, the replacement of Sn^{4+} by In^{3+} ions could be expressed as

$$In_2O_3 \xrightarrow{SnO_2} 2In_{Sn}^{-} + V_O^{gg} + 2O_O^{\times} + \frac{1}{2}O_2$$

where In_{Sn}^{-} represents In substitution in Sn sites, V_O^{gg} represents lattice oxygen vacancies, and $O_O^{\times}$ represents interstitial oxygen. Thus in such a way, the sensor performance will be promoted by adding some In in SnO_2 nanofibers finally. Pd is a traditional dopant for SnO_2, and it has been widely reported for its sensing improvement to H_2, C_2H_5OH, and CH_4, etc. It is accepted that Pd dopant in its oxidized state (PdO) acts as a strong acceptor for electrons of the host semiconductor.[9] This induces an electron-depleted space-charge layer near the interface. By reacting with reducing gas molecules PdO is reduced, releasing the electrons back to the semiconductor, and these phenomena will lead to a high sensitivity of the sensing materials. Co can support the catalytic conversion of CH_4 into its oxidation products, which is due to spill-over of activated fragments to the semiconductor surface to react with the adsorbed oxygen and is called the chemical sensitization. This effect will accelerate the sensing reaction on the fiber surface effectively.

In summary, micro-sensors with a tiny size are fabricated by spinning In-Pd-Co-SnO_2 composite nanofibers on Si substrates. Excellent CH_4 sensing properties are obtained at 140℃. The sensitivity is up to 13 when the sensors are exposed to 10 ppm CH_4, and the response time and recovery times are 8 and 14 s, respectively. The sensors also exhibit high selectivity, good stability, and low power-consumption.

References

[1] Schiermeier Q 2006 *Nature* **439** 128
[2] Liu L, Zhang T, Wang Z J, Li S C, Tian Y X and Li W 2009 *Chin. Phys. Lett.* **26** 090701
[3] Qiu C J, Dou Y W, Zhao Q L, Qu W, Yuan J, Sun Y M and Cao M S 2008 *Chin. Phys. Lett.* **25** 3590
[4] Yue X J, Hong T S, Xu X and Li Z 2011 *Chin. Phys. Lett.* **28** 090701
[5] Xu L, Wang R, Xiao Q, Zhang D and Liu Y 2011 *Chin. Phys. Lett.* **28** 070702
[6] Chen Y J, Nie L, Xue X Y, Wang Y G and Wang T H 2006 *Appl. Phys. Lett.* **88** 083105
[7] Janata J, Josowicz M and Devaney D M 1994 *Anal. Chem.* **66** 207
[8] Qi Q, Zhang T, Liu L, Zheng X, Yu Q, Zeng Y and Yang H 2008 *Sens. Actuators* B **134** 166
[9] Franke M E, Koplin T J and Simon U 2006 *Small* **2** 36
[10] Xu L, Wang R, Liu Y and Dong L 2011 *Chin. Phys. Lett.* **28** 040701
[11] Zhang Y, Li J, An G and He X 2010 *Sens. Actuators* B **144** 43